© 2015. Published by The Company of Biologists Ltd | Development (2015) 142, 3845-3858 doi:10.1242/dev.125542

RESEARCH ARTICLE

A local difference in Hedgehog signal transduction increases mechanical cell bond tension and biases cell intercalations along the *Drosophila* anteroposterior compartment boundary

Katrin Rudolf[1], Daiki Umetsu[2], Maryam Aliee[3], Liyuan Sui[1], Frank Jülicher[3,*] and Christian Dahmann[1,*]

ABSTRACT

Tissue organization requires the interplay between biochemical signaling and cellular force generation. The formation of straight boundaries separating cells with different fates into compartments is important for growth and patterning during tissue development. In the developing *Drosophila* wing disc, maintenance of the straight anteroposterior (AP) compartment boundary involves a local increase in mechanical tension at cell bonds along the boundary. The biochemical signals that regulate mechanical tension along the AP boundary, however, remain unknown. Here, we show that a local difference in Hedgehog signal transduction activity between anterior and posterior cells is necessary and sufficient to increase mechanical tension along the AP boundary. This difference in Hedgehog signal transduction is also required to bias cell rearrangements during cell intercalations to keep the characteristic straight shape of the AP boundary. Moreover, severing cell bonds along the AP boundary does not reduce tension at neighboring bonds, implying that active mechanical tension is upregulated, cell bond by cell bond. Finally, differences in the expression of the homeodomain-containing protein Engrailed also contribute to the straight shape of the AP boundary, independently of Hedgehog signal transduction and without modulating cell bond tension. Our data reveal a novel link between local differences in Hedgehog signal transduction and a local increase in active mechanical tension of cell bonds that biases junctional rearrangements. The large-scale shape of the AP boundary thus emerges from biochemical signals inducing patterns of active tension on cell bonds.

KEY WORDS: Cell sorting, Compartment boundary, Hedgehog, Mechanical tension, *Drosophila*

INTRODUCTION

During development, cells with similar fates often stay together and separate from cells with different fates. The links between cell fate determination and the physical mechanisms guiding cell separation, however, remain unknown. A feature of many developing tissues is the separation of cells with distinct fates or functions into compartments (Vincent, 1998; McNeill, 2000; Irvine and Rauskolb, 2001; Tepass et al., 2002; Blair, 2003; Vincent and Irons, 2009; Martin and Wieschaus, 2010; Dahmann et al., 2011; Monier et al., 2011; Batlle and Wilkinson, 2012). Boundaries between compartments are characterized by a straight morphology. These boundaries are lineage restrictions resulting from a mechanism that prevents the intermingling of adjacent cell populations caused by cell proliferation and cell rearrangements. Signaling across compartment boundaries sets up local organizers along the boundary that instruct growth and patterning throughout the tissue. Maintaining a straight boundary shape between compartments ensures the stable and precise positioning of these organizers during tissue development (Dahmann and Basler, 1999). Compartment boundaries thus serve an important role in tissue growth and patterning.

The *Drosophila* wing imaginal disc (wing disc) serves as a useful model in which to study compartment boundaries. The wing disc is a single-layered epithelium that is set aside during embryonic development, proliferates during larval stages and is reshaped during pupal metamorphosis to give rise to the adult wing (Cohen, 1993). The wing disc is subdivided from embryonic stages onwards into anterior and posterior compartments (Garcia-Bellido et al., 1973). A second compartment boundary, separating cells from the dorsal and ventral compartments, is formed later during larval development (Bryant, 1970; Garcia-Bellido et al., 1973, 1976). The maintenance of the straight shape of the compartment boundary separating anterior and posterior cells (AP boundary) requires the homeodomain-containing proteins Engrailed and Invected (Morata and Lawrence, 1975). Engrailed and Invected are expressed in all posterior cells and specify a posterior-type cell fate. The absence of Engrailed and Invected in anterior cells specifies their anterior-type cell fate. Engrailed and Invected influence boundary shape by two distinct pathways. First, Engrailed and Invected induce expression of the short-range signaling molecule Hedgehog in posterior cells and at the same time repress transcription of the Hedgehog-activated transcription factor Cubitus interruptus (Ci) (Eaton and Kornberg, 1990; Tabata et al., 1992; Zecca et al., 1995). As a consequence, Hedgehog signal transduction is confined to a strip of anterior cells along the AP boundary. Transduction of the Hedgehog signal is required for A cells to separate from P cells (Hedgehog-dependent pathway) (Blair and Ralston, 1997; Rodriguez and Basler, 1997; Dahmann and Basler, 2000). Second, Engrailed and Invected contribute to the characteristic straight shape of the AP boundary independently of Hedgehog signal transduction (Hedgehog-independent pathway) (Blair and Ralston, 1997; Dahmann and Basler, 2000). The mechanism(s) by which the Hedgehog-dependent and Hedgehog-independent pathways influence the shape of the AP boundary remain elusive.

Recent work has shed light on the physical mechanisms that maintain the straight shape of compartment boundaries. Cell junctions along compartment boundaries in *Drosophila* and vertebrate embryos show increased levels of F-actin and non-

[1]Institute of Genetics, Technische Universität Dresden, Dresden 01062, Germany. [2]RIKEN Center for Developmental Biology, Kobe 650-0047, Japan. [3]Max Planck Institute for the Physics of Complex Systems, Nöthnitzer Strasse 38, Dresden 01187, Germany.

*Authors for correspondence (julicher@pks.mpg.de; christian.dahmann@tu-dresden.de)

Received 23 April 2015; Accepted 24 September 2015

Development (2015) 142, 3845-3858 doi:10.1242/dev.125542

muscle Myosin II (Myosin II) (Major and Irvine, 2005, 2006; Landsberg et al., 2009; Monier et al., 2010; Aliee et al., 2012; Calzolari et al., 2014). It has been proposed that F-actin and Myosin II form an actomyosin cable along the compartment boundary that acts as a fence preventing the mixing of cells from adjacent compartments (Major and Irvine, 2005, 2006; Monier et al., 2010; Calzolari et al., 2014). However, whether this cable acts like an elastic string or whether mechanical tension is rather generated locally at each cell bond independently of the overall integrity of the cable remains unknown.

Our previous work has demonstrated that mechanical tension at adherens junctions (termed cell bond tension) is increased along the AP and dorsoventral (DV) boundaries compared with the bulk of the wing disc (Landsberg et al., 2009; Aliee et al., 2012). Cell bond tension results from the activity of Myosin II on F-actin and other contractile elements associated with cell junctions and cell adhesion. Simulations of tissue growth with two compartments furthermore suggest that such local increases in cell bond tension can prevent cell mixing between two adjacent cell populations and can account for the straight shape of compartment boundaries (Landsberg et al., 2009; Aliee et al., 2012). Consistent with these data, reducing Myosin II activity, either throughout the tissue or locally along the compartment boundary, compromises boundary shape (Major and Irvine, 2006; Landsberg et al., 2009; Monier et al., 2010; Aliee et al., 2012; Calzolari et al., 2014). Recent data suggest that local increases in cell bond tension bias cell rearrangements to maintain the straight shape of compartment boundaries (Umetsu et al., 2014). The signals that result in the local increase in cell bond tension along compartment boundaries, however, are not known. It has been proposed that local increases in cell bond tension result from Hedgehog signaling across the AP boundary (Landsberg et al., 2009; Schilling et al., 2011).

Here, we demonstrate that the difference in Hedgehog signal transduction activity between anterior and posterior cells is necessary and sufficient to increase cell bond tension along the AP boundary and is required to bias cell rearrangements during cell intercalations along the AP boundary. Moreover, cutting the actomyosin cable with a laser beam does not affect cell bond tension along the AP boundary, suggesting that mechanical tension is generated locally at each cell bond independently of the overall integrity of the cable. Finally, the Hedgehog-independent pathway, although contributing to the straight shape of the AP boundary, apparently does not influence cell bond tension. Our work demonstrates a link between Hedgehog signal transduction, increased cell bond tension and biased cell intercalations that is important for shaping the AP boundary. Moreover, we reveal a second mechanism that does not involve tension increases and that further contributes to the characteristic straight shape of the AP boundary.

RESULTS

Hedgehog is required to maintain the straight shape of the AP boundary

The compartment boundary separating anterior and posterior cells of the larval wing disc is characterized by a straight and sharp morphology (Landsberg et al., 2009). Mosaic analysis has shown that Hedgehog signal transduction is required in anterior cells for them to remain separate from posterior cells (Blair and Ralston, 1997; Rodriguez and Basler, 1997; Dahmann and Basler, 2000). Mutant clones of cells located along the compartment boundary were given the choice whether to segregate from anterior cells, posterior cells, or both. These experiments, therefore, revealed the sorting preference of mutant clones of cells with respect to surrounding wild-type cells. They did not, however, address the question of whether or not Hedgehog signal transduction is required to maintain the straight shape of the AP boundary during wing disc development.

Hedgehog protein is expressed in cells of the posterior compartment (Tabata et al., 1992); however, these cells do not transduce the Hedgehog signal owing to a lack of the transcription factor Cubitus interruptus (Ci), which is required for Hedgehog target gene expression (Dominguez et al., 1996). Hedgehog secreted from posterior cells moves to cells of the anterior compartment, which receive and transduce the signal resulting in changes in gene expression (Basler and Struhl, 1994; Tabata and Kornberg, 1994). Hedgehog spreads only a limited distance throughout the anterior compartment resulting in a strip along the AP boundary of approximately ten cells wide that transduces the Hedgehog signal (Chen and Struhl, 1996). We first tested whether Hedgehog activity is required to maintain the straight shape of the AP boundary. To reduce Hedgehog activity, we used a temperature-sensitive allele of hedgehog (hh^{ts2}) (Ma et al., 1993). In homozygous hh^{ts2} mutant larvae reared at the restrictive temperature for 24-26 h, expression of *ptc*, a Hedgehog target gene (Forbes et al., 1993), was no longer detectable (Fig. S1A,B), showing that Hedgehog signal transduction was greatly reduced under these conditions. Wing discs were immunostained for E-cadherin (Shg – FlyBase) to mark cellular adherens junctions and posterior cells were labeled using the *engrailed-lacZ* enhancer trap line (Hama et al., 1990) to identify the AP boundary. The shape of the AP boundary was characterized by a geometric measure termed roughness (Fig. S4; supplementary materials and methods) (Landsberg et al., 2009). The roughness w describes the variance of the distance of a boundary from a straight line as a function of the length L of the boundary segment that is analyzed (Fig. 1A). The dependence of roughness w on segment length L reveals the scaling behavior of the interface morphology (Barabasi and Stanley, 1995). In control wing discs, the roughness of the AP boundary increased with the segment length L of the boundary analyzed (Fig. 1C,E,F). In homozygous hh^{ts2} mutants at the restrictive temperature, the roughness of the AP boundary also increased with increasing length of the boundary segment, but was greater than in control wing discs for all segment lengths L analyzed (Fig. 1D,E,G). These results show that Hedgehog is required to maintain the straight morphology characteristic of the AP boundary.

Hedgehog is required for the local increase in cell bond tension along the AP boundary

The straight and sharp morphology of the AP boundary involves a local increase in cell bond tension (Landsberg et al., 2009). The local increase in cell bond tension along the AP boundary correlates with morphological and molecular signatures, including the enrichment of F-actin and Myosin II at adherens junctions and wider angles between adjacent cell bonds along the AP boundary compared with angles between adjacent cell bonds away from the AP boundary (Landsberg et al., 2009). We first tested whether these morphological and molecular signatures of the AP boundary depended on Hedgehog activity. Compared with controls, in homozygous hh^{ts2} mutant wing discs, the angle between adjacent cell bonds along the AP boundary was no longer widened (Fig. 1B,H). Moreover, an enlarged apical cross-section area of cells located along the AP boundary (compared with cells elsewhere), a further characteristic of the AP boundary (Landsberg et al., 2009), was no longer observed in homozygous hh^{ts2} mutants (Fig. 1B,I). Finally, F-actin and Myosin II [as visualized by Myosin Regulatory Light Chain (MRLC)-GFP] was no longer enriched at adherens junctions along the AP boundary in

Development (2015) 142, 3845-3858 doi:10.1242/dev.125542

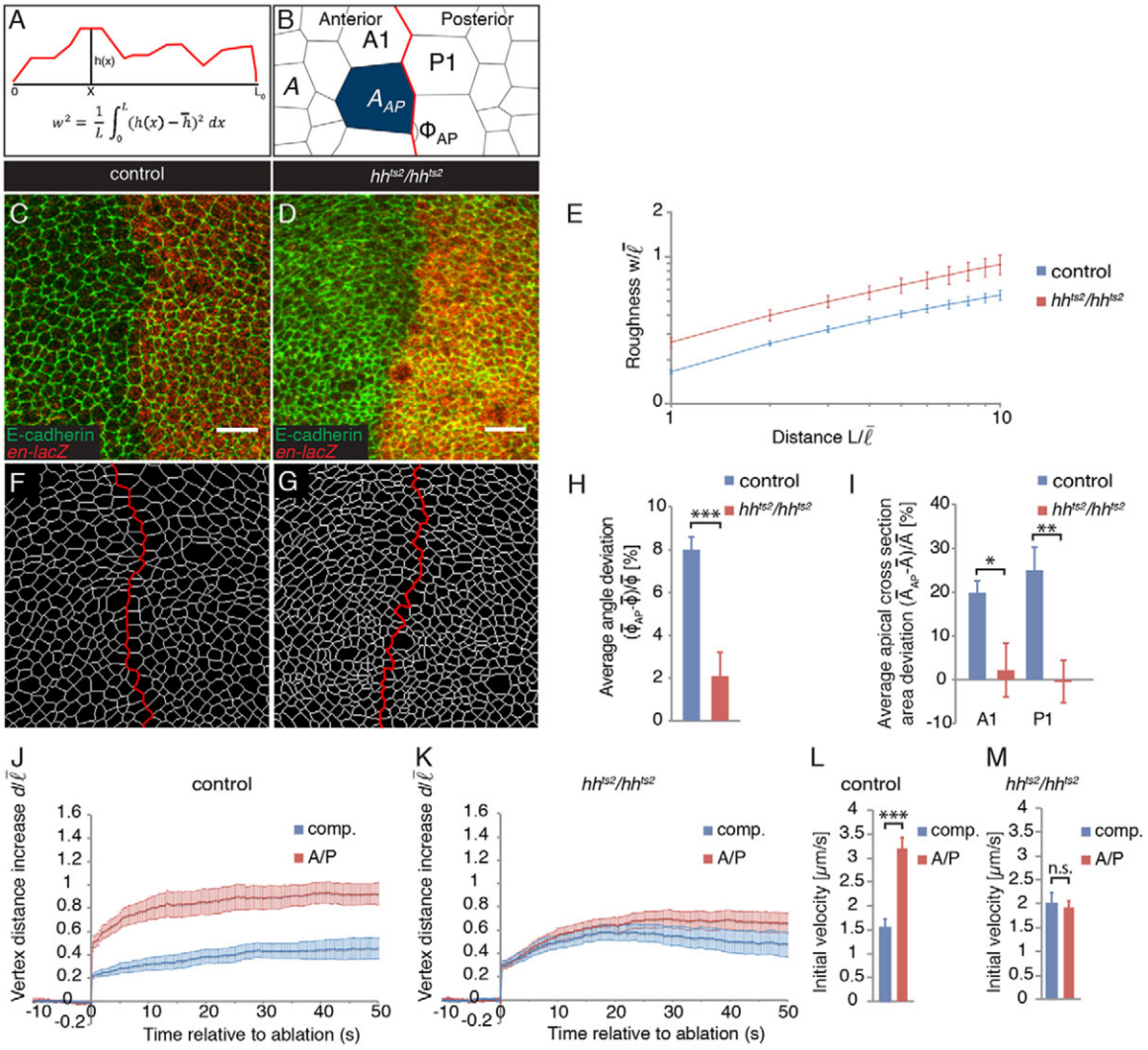

Fig. 1. Hedgehog is required for the local increase in cell bond tension along the AP boundary. (A) Scheme depicting the measurement of roughness *w* of a boundary. For any distance *L* along a boundary, h(x) describes the shape of the boundary line (red line) (see supplementary materials and methods). (B) Red line indicates the compartment boundary. A1 and P1 refer to the first row of anterior and posterior cells along the AP boundary, respectively. Apical cross-section area of cells away from (*A*) and along (A_{AP}) the AP boundary and the angle between neighboring cell bonds (ϕ_{AP}) along the AP boundary are depicted. (C,D) Wing discs of control hh^{ts2}/+ (C) and homozygous hh^{ts2}/hh^{ts2} mutant (D) larvae raised for 24-26 h at 29°C stained for E-cadherin (green) and the activity of *en-lacZ* (red). Scale bars: 10 µm. (E) Roughness *w* of the AP boundary for the distances *L* for the genotypes shown in C,D. Distance and roughness values are normalized by the average cell bond length in the tissue $\bar{\ell} = 1.7$ µm . Mean and s.e.m. are shown (control, *n*=6 wing discs; mutant, *n*=7 wing discs). *P*<0.01-0.05 for all distances shown. (F,G) Segmentations of the images shown in C and D, respectively. Red lines indicate AP boundary. (H) Difference of the average angle between neighboring cell bonds along the AP boundary $\bar{\phi}_{AP}$ and the average angle between cell bonds in the tissue $\bar{\phi} = 119.8°$ (normalized to $\bar{\phi}$) as a percentage for wing discs of the indicated genotypes. Mean and s.e.m. are shown (control, *n*=6 wing discs; mutant, *n*=4 wing discs). ***P*<0.001. (I) Difference in the average apical cross-section area of A1 or P1 cells, $\bar{A}_{AP}$, and the average apical cross section area of cells in the tissue $\bar{A} = 4.8$ µm^2 (normalized to $\bar{A}$) as a percentage for wing discs of the indicated genotypes. Mean and s.e.m. are shown (control, *n*=6 wing discs; mutant, *n*=8 wing discs). **P*<0.05; ***P*<0.01. (J,K) Change in distance *d* between the vertices of cell bonds located within the compartments (comp.) or at the AP boundary after ablation (normalized to $\bar{\ell}$) as a function of time for wing discs of control and homozygous hh^{ts2} mutant larvae raised for 24-26 h at 29°C. Mean and s.e.m. are shown [control, *n*=10 (comp.), *n*=10 (A/P) cuts; mutant, *n*=16 (comp.), *n*=19 (A/P) cuts]. (L,M) Initial velocity of vertex displacement after ablation of the indicated types of cell bonds for control (L) and homozygous hh^{ts2} mutant (M) larvae raised for 24-26 h at 29°C. Mean and s.e.m. are shown (*n* as in J,K). ***P*<0.001; n.s., not significant.

homozygous hh^{ts2} mutants (Fig. S2A-F). Thus, Hedgehog activity is required for the enrichment of F-actin and Myosin II, and for widened angles between cell bonds along the AP boundary, all of which are signatures of local increases in cell bond tension.

Ablation of individual cell bonds creates tissue relaxations that are direct and quantitative indicators of cell bond tension (Farhadifar et al., 2007). Cell bonds were identified using E-cadherin-GFP (Huang et al., 2009) and the posterior compartment was labeled by expression of a membrane-linked form of GFP (GFP-gpi) under control of an *en-GAL4* driver line. We ablated individual cell bonds in wing discs using a laser beam and quantified the resulting displacement of the two vertices of the ablated cell bond by live imaging. The maximal increase in distance between vertices (final vertex displacement) resulting from ablation of cell bonds located away from the AP boundary was comparable between control wing discs and wing discs of homozygous hh^{ts2} mutants (Fig. 1J,K; Fig. S3A). Moreover, in control wing discs, the final vertex displacement was increased for cell bonds along the AP boundary compared with cell bonds away from the AP boundary (Fig. 1J), as described previously (Landsberg et al., 2009). Remarkably, in wing

Development (2015) 142, 3845-3858 doi:10.1242/dev.125542

discs of homozygous hh^{ts2} mutants, the final vertex displacement upon ablation of cell bonds along the AP boundary was indistinguishable from the displacement of cell bonds away from the boundary (Fig. 1K). The ratio of the initial velocities of vertex displacement upon ablation of cell bonds is a quantitative measure of the ratio of tension on these cell bonds (Mayer et al., 2010). The initial velocity of vertex displacement upon ablation of cell bonds along the AP boundary was in control wing discs approximately twofold higher compared with the initial velocity of vertex displacement upon ablation of cell bonds elsewhere in the tissue (Fig. 1L; Landsberg et al., 2009). By contrast, in wing discs of homozygous hh^{ts2} mutants the initial velocities of vertex displacement were similar upon ablation of cell bonds along the AP boundary and cell bonds elsewhere (Fig. 1M). These results demonstrate that the local increase in cell bond tension along the AP boundary depends on Hedgehog activity.

Differences in Hedgehog signal transduction are required to increase cell bond tension locally along the AP boundary

Cells located on the two sides of the AP boundary differ in their Hedgehog signal transduction activities. Anterior cells close to the AP boundary transduce the Hedgehog signal whereas posterior cells do not (Zecca et al., 1995). We tested whether this difference in Hedgehog signal transduction between anterior and posterior cells is required to maintain the straight shape of the AP boundary, the morphological and molecular characteristics of cells along the AP boundary, and the local increase of cell bond tension at the AP boundary. To this end, we sought to increase Hedgehog signal transduction in posterior cells by expressing in these cells an activated form of the transcription factor Ci (Ci^{PKA4}) that is sufficient to activate Hedgehog target genes in the absence of Hedgehog ligand (Methot and Basler, 2000). As a consequence, *ptc-lacZ* and *dpp-lacZ*, two reporters of Hedgehog signal transduction (Blackman et al., 1991; Forbes et al., 1993), were expressed in posterior cells (Fig. S1C-F), indicating that the difference in Hedgehog signal transduction between anterior and posterior cells was reduced under these conditions. The roughness of the AP boundary was increased in the wing discs expressing Ci^{PKA4} in the posterior compartment compared with controls (Fig. 2A-E). Moreover, in these wing discs the angle between adjacent cell bonds was no longer widened (Fig. 2F), cells along the AP boundary no longer had an enlarged apical cross-section area (Fig. 2G) and F-actin was no longer enriched at adherens junctions along the AP boundary (Fig. S2G-I). Lastly, we analyzed the cell bond tension along the AP boundary in wing discs expressing Ci^{PKA4} in the posterior compartment. The final vertex displacement upon ablation of cell bonds along the AP boundary in these wing discs was similar to the final vertex displacement upon ablation of cell bonds elsewhere (Fig. 2H; Fig. S3B). The initial velocities of vertex displacement upon ablation of cell bonds along the AP boundary and cell bonds elsewhere in wing discs expressing Ci^{PKA4} were similar (Fig. 2I). We conclude that the difference in Hedgehog signal transduction between anterior and posterior cells is required for the morphological and molecular features that are characteristic of cells along the AP boundary, for the characteristic straight shape of the AP boundary, and for locally increasing cell bond tension.

Differences in Hedgehog signal transduction are sufficient to increase cell bond tension locally along the AP boundary

We next tested whether the difference in Hedgehog signal transduction between anterior and posterior cells is sufficient to maintain the straight shape of the AP boundary, the morphological and molecular characteristics of cells along the AP boundary, and the local increase of cell bond tension at the AP boundary. We sought to create a scenario in which the Hedgehog signal is no longer transduced in anterior cells, but instead is transduced in posterior cells. To this end, we expressed Ci^{PKA4} in the posterior compartment of wing discs carrying the temperature-sensitive hh^{ts2} allele. At the restrictive temperature, Patched expression was confined to cells of the posterior compartment (Fig. S1G), indicating that the Hedgehog signal was only transduced in these cells. The roughness of the AP boundary was reduced compared with hh^{ts2} mutant wing discs and was comparable to control wing discs (Fig. 3A-C). Moreover, the angle between adjacent cell bonds was widened (Fig. 3D), cells along the AP boundary had an enlarged apical cross-section area (Fig. 3E), and F-actin was enriched at adherens junctions along the AP boundary (Fig. S2J,K). Moreover, the final vertex displacement upon ablation of cell bonds along the AP boundary in these wing discs was increased compared with the final vertex displacement upon ablation of cell bonds elsewhere in the wing disc (Fig. 3F; Fig. S3C). The initial velocities of vertex displacement upon ablation of cell bonds along the AP boundary were increased at least twofold compared with cell bonds elsewhere in wing discs (Fig. 3G), comparable to observations in control wing discs. We conclude that a difference in Hedgehog signal transduction between anterior and posterior cells is sufficient for the morphological and molecular features that are characteristic of cells along the AP boundary, for the characteristic straight shape of the AP boundary, and for locally increasing cell bond tension.

Differences in Hedgehog signal transduction across clone borders are sufficient to increase cell bond tension locally

We next tested whether a difference in Hedgehog signal transduction between adjacent cell populations within one compartment of wing discs is sufficient to induce a smooth interface, the morphological and molecular characteristics of cells seen along the AP boundary, and a local increase of cell bond tension. We generated clones of marked cells that constitutively transduced the Hedgehog signal by expression of Ci^{PKA4} and analyzed these clones in the posterior compartment of the wing disc, an area that does not normally transduce the Hedgehog signal. In contrast to the ragged border of control clones, clones expressing Ci^{PKA4} had smooth borders (Fig. 4C,D). We characterized the morphology of the clones by a geometric measure termed ‘clonal roughness’. Clonal roughness describes the roughness of the clone boundary taking into account that the clone boundary is not on average straight but curved (Fig. 4A; Fig. S5; supplementary materials and methods). The clonal roughness of Ci^{PKA4}-expressing clones was lower compared with the clonal roughness of control clones (Fig. 4E-G). Moreover, angles between adjacent cell bonds along the clone border were larger compared with control clones (Fig. 4B,H) and the apical cross-section area of cells located along the border of Ci^{PKA4}-expressing clones was larger compared with control clones (Fig. 4I). Furthermore, F-actin was enriched along borders of Ci^{PKA4}-expressing clones but not control clones (Fig. S2L-N). Lastly, we analyzed the vertex displacement upon ablation of cell bonds at the border of control clones and clones expressing Ci^{PKA4} and compared it with the vertex displacements of cell bonds located along or away from the AP boundary. The final vertex displacement upon ablation of cell bonds along control clones was similar to the final vertex displacement upon ablation of cell bonds between two anterior cells (Fig. 4J; Fig. S3D). The final vertex displacement upon ablation of cell bonds along borders of Ci^{PKA4}-expressing clones was larger compared with control clones

Development (2015) 142, 3845-3858 doi:10.1242/dev.125542

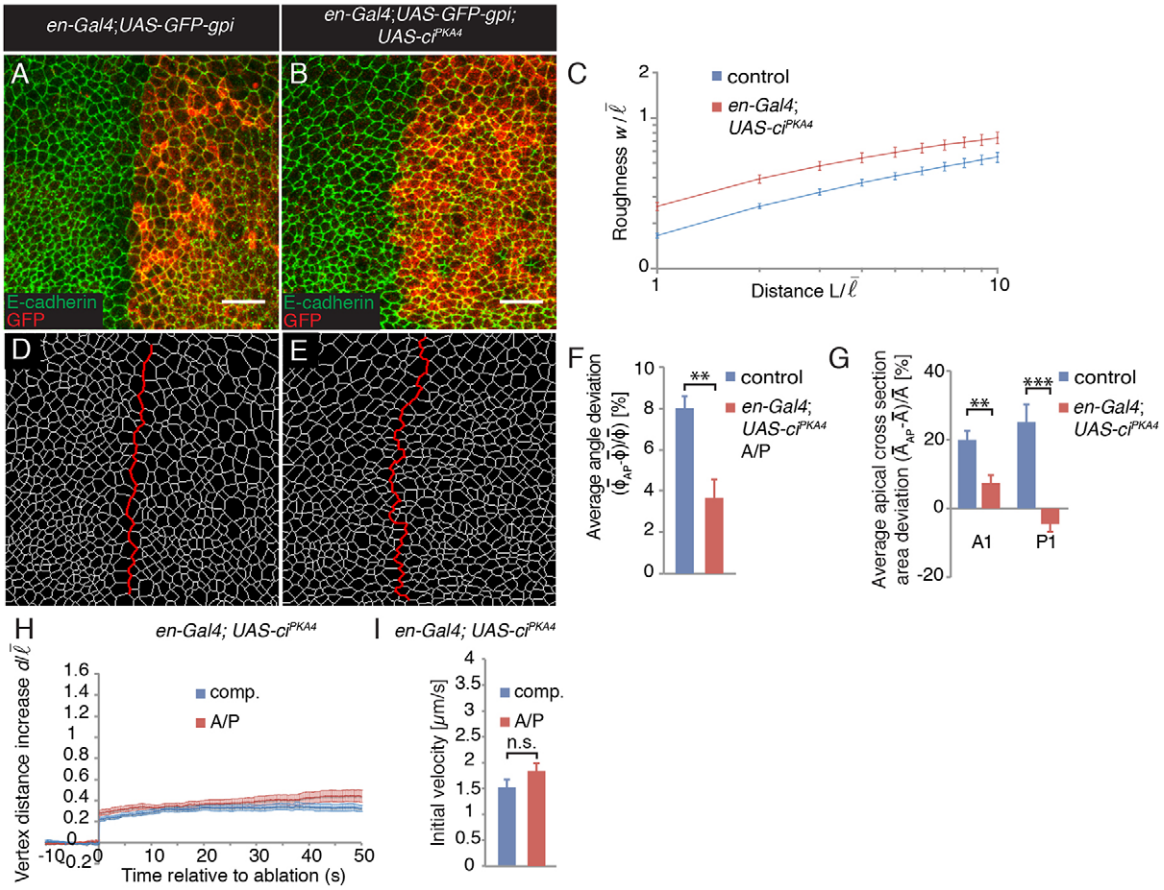

Fig. 2. Differences in Hedgehog signal transduction are required to increase cell bond tension locally along the AP boundary. (A,B) Control wing discs expressing GFP-gpi (A; *en-Gal4*; *UAS-GFP-gpi*) and wing discs co-expressing GFP-gpi and Ci^{PKA4} in the posterior compartment (B; *en-Gal4*; *UAS-GFP-gpi*; *UAS-ci*^{PKA4}) stained for E-cadherin (green) and GFP (red). Scale bars: 10 µm. (C) Roughness w of the AP boundary for the distances L for the genotypes shown in A,B. Mean and s.e.m. are shown (control, n=6 wing discs; mutant, n=7 wing discs). P<0.01-0.05 for all distances shown. (D,E) Segmentations of the images shown in A and B, respectively. Red lines indicate AP boundary. (F) Difference of the average angle between neighboring cell bonds along the AP boundary $\bar{\phi}_{AP}$ and the average angle between cell bonds in the tissue $\bar{\phi} = 119.8°$ (normalized to $\bar{\phi}$) as a percentage for wing discs of the indicated genotypes. Mean and s.e.m. are shown (control, n=6 wing discs; mutant, n=7 wing discs). **P<0.01. (G) Difference in the average apical cross-section area of A1 or P1 cells, $\bar{A}_{AP}$, and the average apical cross section area of cells in the tissue $\bar{A} = 4.8\ \mu m^2$ (normalized to $\bar{A}$) as a percentage for wing discs of the indicated genotypes. Mean and s.e.m. are shown (control, n=6 wing discs; mutant, n=5 wing discs). **P<0.01; ***P<0.001. (H) Change in distance d between the vertices of cell bonds located within the compartments (comp.) or at the AP boundary after ablation as a function of time for wing discs of the indicated genotype. Mean and s.e.m. are shown [n=14 (comp), n=15 (A/P) cuts]. (I) Initial velocity of vertex displacement after ablation of the indicated types of cell bonds for wing discs of the indicated genotypes. Mean and s.e.m. are shown (n as in H). n.s., not significant.

and was nearly as large as the final vertex displacement upon ablation of cell bonds along the AP boundary (Fig. 4J). The initial velocities of vertex displacement upon ablation of cell bonds along Ci^{PKA4}-expressing clones and cell bonds along the AP boundary were similar and approximately twofold higher compared with the initial velocities of vertex displacement upon ablation of cell bonds at borders of control clones or cell bonds away from the AP boundary (Fig. 4K). We conclude that a difference in Hedgehog signal transduction between adjacent cell populations within a compartment is sufficient to induce morphological and molecular features that are characteristic of cells along the AP boundary and to increase cell bond tension locally.

Increased mechanical tension along the AP boundary is generated autonomously at each cell bond

How does a difference in Hedgehog signal transduction between anterior and posterior cells lead to an increased cell bond tension along the AP boundary? The difference in Hedgehog signal transduction results in increased amounts of F-actin and Myosin II that have been observed along compartment boundaries and that have been termed ‘actomyosin cable’ (Major and Irvine, 2005, 2006; Monier et al., 2010; Calzolari et al., 2014). This term highlights the multicellular aspect of this contractile structure and might suggest that increased cell bond tension is a collective property of multiple cells along the AP boundary. Alternatively, the local difference in Hedgehog signal transduction across the AP boundary could locally trigger an increase in tension, cell bond by cell bond. To begin to distinguish between these two possibilities, we activated Hedgehog signal transduction in single cells by expressing Ci^{PKA4} (Fig. S1H) and measured the mechanical tension at cell bonds between a Ci^{PKA4}-expressing cell and its neighboring control cells in the posterior compartment (Fig. 5A). The final vertex displacement upon ablation of cell bonds between a Ci^{PKA4}-expressing cell and its neighbors was larger compared with control cells and was comparable to the final vertex displacement upon ablation of cell bonds along the AP boundary (Fig. 5B,C, compare with Fig. 1J; Movie 1). The initial velocities of vertex displacement upon ablation of cell bonds between a Ci^{PKA4}-expressing cell and its

Development (2015) 142, 3845-3858 doi:10.1242/dev.125542

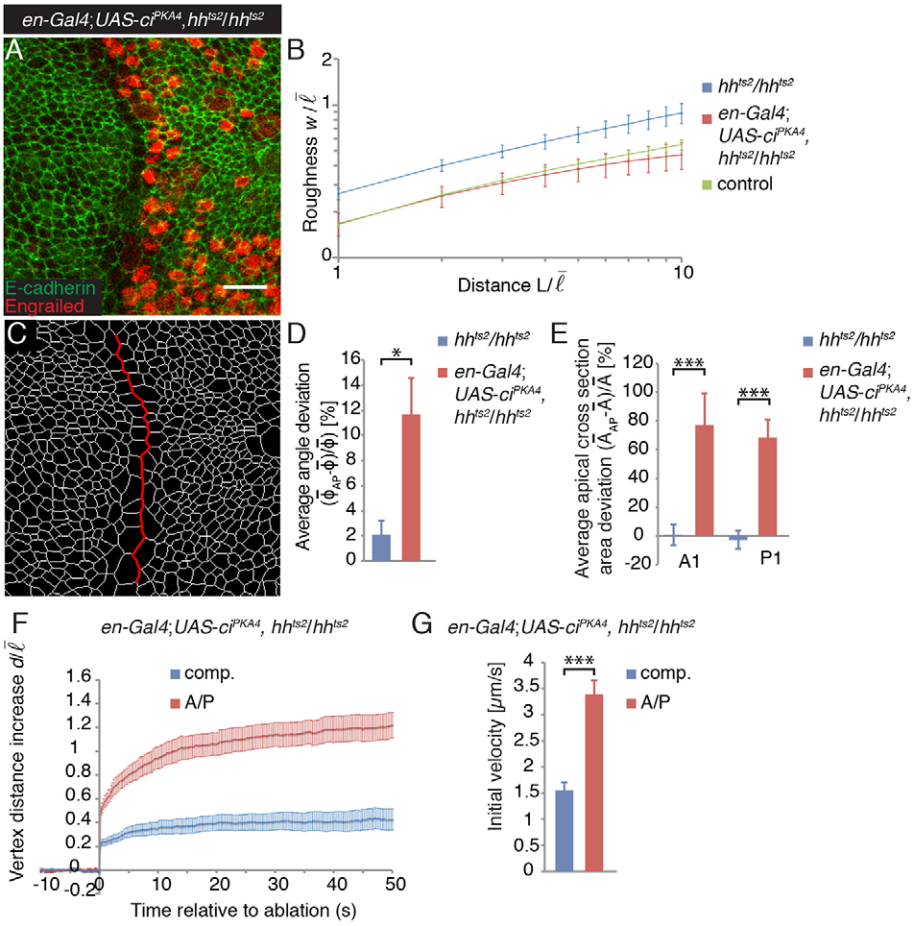

Fig. 3. Differences in Hedgehog signal transduction are sufficient to increase cell bond tension locally along the AP boundary. (A) Wing discs of homozygous hh^{ts2} mutant larvae raised for 24-26 h at 29°C expressing Ci^{PKA4} in the posterior compartment (*en-Gal4*; *UAS-ci*^{PKA4}, hh^{ts2}/hh^{ts2}) stained for E-cadherin (green) and Engrailed (red). Scale bar: 10 µm. (B) Roughness *w* of the AP boundary for the distances *L* for the indicated genotypes. Mean and s.e.m. are shown [hh^{ts2}/hh^{ts2}, *n*=7 wing discs; *en-Gal4; UAS-ci*^{PKA4}, hh^{ts2}/hh^{ts2}, *n*=5 wing discs; control (hh^{ts2}/+), *n*=6 wing discs]; for *en-Gal4*; *UAS-ci*^{PKA4}, hh^{ts2}/hh^{ts2} compared with hh^{ts2}/hh^{ts2}: $P<0.05$ for all distances shown; for *en-Gal4*; *UAS-ci*^{PKA4}, hh^{ts2} compared with hh^{ts2}/+ (control): $P>0.05$ for all distances shown. (C) Segmentation of the image shown in A. Red line indicates AP boundary. (D) Difference of the average angle between neighboring cell bonds along the AP boundary $\bar{\phi}_{AP}$ and the average angle between cell bonds in the tissue $\bar{\phi} = 119.8°$ (normalized to $\bar{\phi}$) as a percentage for wing discs of the indicated genotypes. Mean and s.e.m. are shown (hh^{ts2}/hh^{ts2}, *n*=4 wing discs; *en-Gal4; UAS-ci*^{PKA4}, hh^{ts2}/hh^{ts2}, *n*=4 wing discs). *$P<0.05$. (E) Difference in the average apical cross-section area of A1 and P1 cells, $\bar{A}_{AP}$, and the average apical cross-section area of cells in the tissue $\bar{A} = 4.8\ \mu m^2$ (normalized to $\bar{A}$) as a percentage for wing discs of the indicated genotypes. Mean and s.e.m. are shown (hh^{ts2}/hh^{ts2}, *n*=8 wing discs; *en-Gal4; UAS-ci*^{PKA4}, hh^{ts2}/hh^{ts2}, *n*=4 wing discs). ***$P<0.001$. (F) Change in distance *d* between the vertices of cell bonds located within the compartments (comp.) or at the AP boundary after ablation as a function of time for wing discs of the indicated genotype. Mean and s.e.m. are shown [*n*=14 (comp.), *n*=15 (A/P)]. (G) Initial velocity of vertex displacement after ablation of the indicated types of cell bonds for wing discs of the indicated genotype. Mean and s.e.m. are shown (*n* as in F). ***$P<0.001$.

neighbors and cell bonds along the AP boundary were similar and were increased compared with the initial velocities of vertex displacement upon ablation of control cell bonds away from the AP boundary (Fig. 5D, compare with Fig. 1L). These results suggest that a difference in Hedgehog signal transduction between two cells is sufficient to increase mechanical tension at the cell bond between these two cells.

To further test whether the local increase of cell bond tension along the AP boundary relies on a multicellular structure or is generated cell bond by cell bond, we subsequently ablated two cell bonds along the AP boundary with a time delay of 20 s (Fig. 5E). The first ablation disrupted the integrity of the cable and the second ablation was used to measure the remaining tension two cell bonds away. We find that both the maximal vertex displacement as well as the initial velocity of vertex displacement was indistinguishable for the first and second ablation events (Fig. 5F-H; Movie 2). These data show that cutting the AP boundary does not lead to a decrease in cell bond tension at the AP boundary in the vicinity of the cut. They suggest that a difference in Hedgehog signal transduction increases mechanical tension autonomously cell bond by cell bond.

Differences in Hedgehog signal transduction bias cell rearrangements during cell intercalations

How do differences in Hedgehog signal transduction activity contribute to the straight shape of the AP boundary? Cell intercalations caused by cell proliferation and tissue remodeling induce irregularities in the shape of compartment boundaries (Umetsu et al., 2014). During cell intercalations (T1 transitions), the shrinkage of a junction between two neighboring cells into a four-way vertex is followed by the generation of a new junction leading to a new pair of cells (Stavans, 1993) (Fig. 5I). The junctional shrinkage during T1 transitions is frequently asymmetric in that one of the two vertices at the end of the shrinking junction moves predominantly (Umetsu et al., 2014). This asymmetric shrinkage of

Development (2015) 142, 3845-3858 doi:10.1242/dev.125542

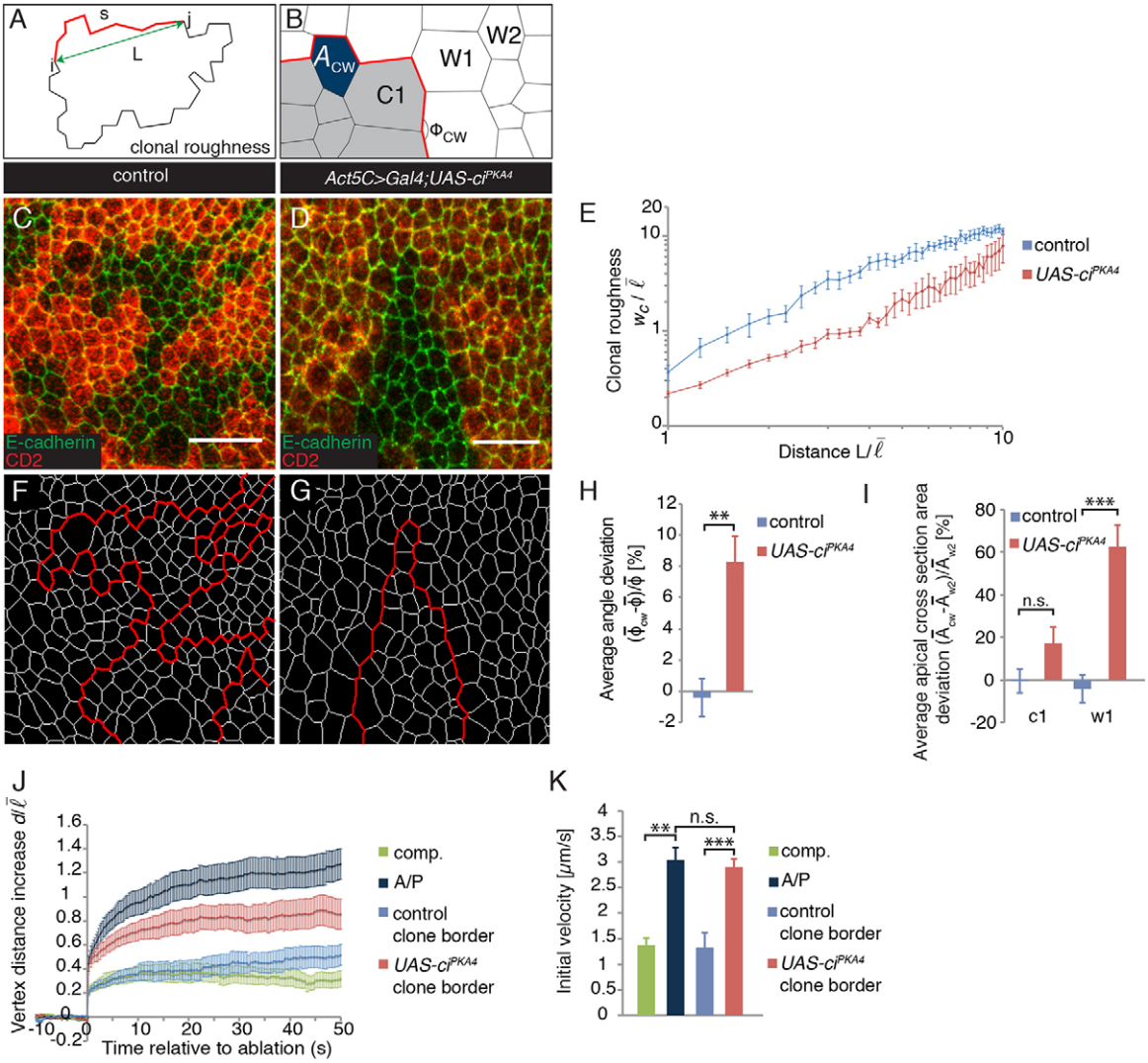

Fig. 4. Differences in Hedgehog signal transduction across clone borders are sufficient to increase cell bond tension locally. (A) Scheme depicting the measurement of clonal roughness. Clonal roughness measures the average variation of contour length *s* between vertices i and j from a straight line for any distance *L* (see supplementary materials and methods). (B) Red line indicates the clone border. The clone is shaded in gray. W1 and W2 refer to the first and second row of cells outside the clone and C1 refers to the first row of cells inside the clone. Apical cross-section area of cells at the clone border, A_{CW}, and the angle between neighboring cell bonds ϕ_{cw} along the clone border are depicted. (C,D) Wing discs displaying control (C; *Act5C<Gal4*) and Ci^{PKA4}-expressing (D; *Act5C<Gal4*, *UAS-Ci*^{PKA4}) clones of cells marked by the absence of CD2 (red). E-cadherin is shown in green. Scale bars: 10 µm. (E) Clonal roughness w_c of the borders of control and Ci^{PKA4}-expressing clones of cells for distances *L*. Distance and roughness values are normalized by the average cell bond length in the tissue $\bar{\ell} = 1.7$ µm. Mean and s.e.m. are shown (control, *n*=7 clones; Ci^{PKA4}, *n*=6 clones). (F,G) Segmentations of the images shown in C and D, respectively. Red lines indicate clone borders. (H) Difference of the average angle between neighboring cell bonds along the clone border $\bar{\phi}_{cw}$ and the average angle between cell bonds in the tissue $\bar{\phi} = 119.8^{\circ}$ (normalized to $\bar{\phi}$) as a percentage for wing discs of the indicated genotypes. Mean and s.e.m. are shown (control, *n*=5 clones; Ci^{PKA4}, *n*=4 clones). ***P*<0.01. (I) Difference in the average apical cross-section area of cells (W1, W2) along the clone border ($\bar{A}_{cw}$) and cells located in the second cell row outside the clones ($\bar{A}_{w2}$), normalized to $\bar{A}_{w2}$ as a percentage for wing discs of the indicated genotypes. Mean and s.e.m. are shown (control, *n*=5 clones; Ci^{PKA4}, *n*=6 clones). ****P*<0.001; n.s., not significant. (J) Change in distance *d* between the vertices of the indicated cell bonds after ablation as a function of time. Mean and s.e.m. are shown (comp., *n*=10; A/P, *n*=12; control clone, *n*=7; Ci^{PKA4}, *n*=12 cuts). (K) Initial velocity of vertex displacement after ablation of indicated cell bonds. Mean and s.e.m. are shown (*n* as in J). ****P*<0.001; ***P*<0.01; n.s., not significant.

junctions is unbiased for T1 transitions in the bulk of the tissue. For T1 transitions in which a new junction is gained along the AP boundary of wing discs, however, the asymmetry of shrinkage is biased. Cell junctions shrink predominantly from the vertex located away from the AP boundary. This bias results in a cell configuration that minimizes irregularities in the shape of the AP boundary (Umetsu et al., 2014). Theoretical considerations of force balances and simulations of tissue growth with two compartments suggest that the bias of asymmetric shrinkage during T1 transitions is a consequence of the local increase in cell bond tension along the AP boundary (Umetsu et al., 2014). We therefore tested whether the difference in Hedgehog signal transduction activity between anterior and posterior cells is required to bias the asymmetric shrinkage of junctions during T1 transitions along the AP boundary. To this end, we again increased Hedgehog signal transduction in posterior cells by expressing in these cells the activated transcription factor Ci^{PKA4}. As shown in Fig. S1D,F, in this scenario Hedgehog signal transduction is active in both anterior and posterior cells. We cultured wing discs, acquired time-lapse movies, and analyzed T1 transitions in which a new junction was gained along the AP

Development (2015) 142, 3845-3858 doi:10.1242/dev.125542

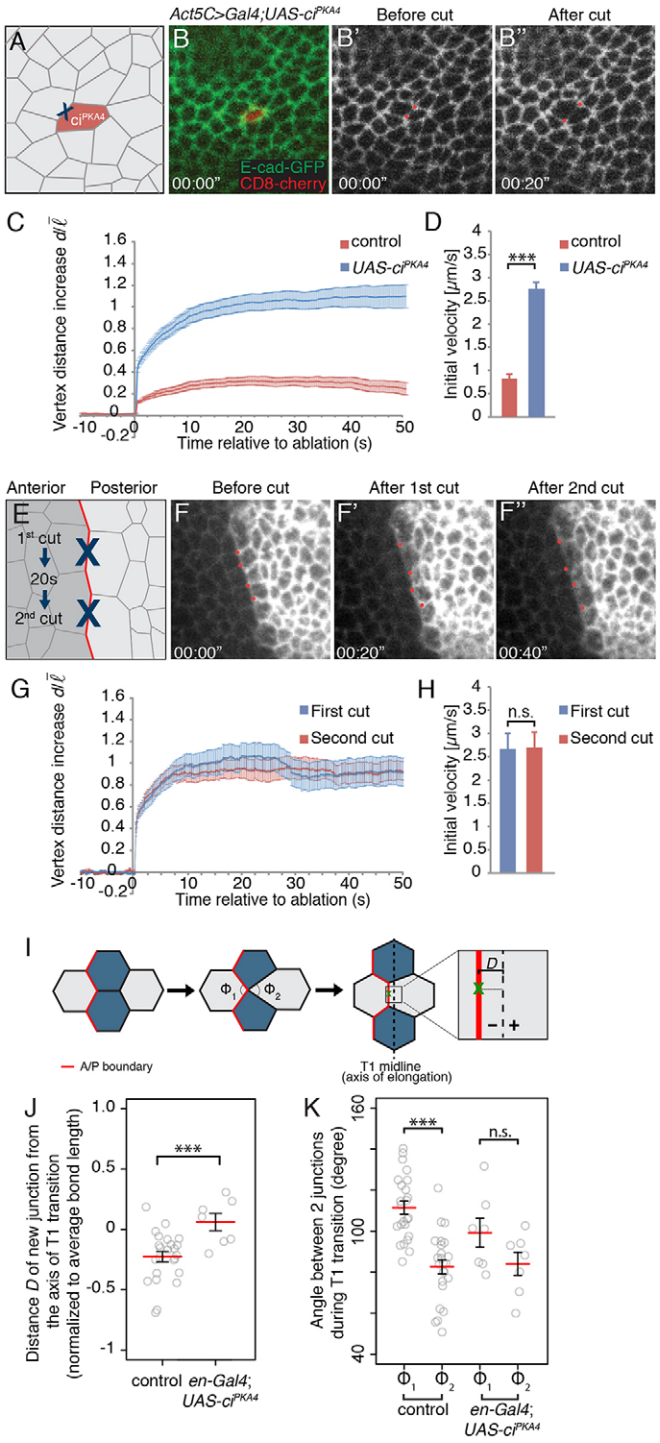

Fig. 5. Increased cell bond tension is generated autonomously and biases cell rearrangements during cell intercalations along the AP boundary. (A) Scheme detailing experimental strategy. Cell bonds between single cells expressing Ci^{PKA4} (red) and its neighbors are ablated (blue cross). (B-B″) Images from a time-lapse movie (Movie 1) immediately before and after laser ablation (times in seconds) of a cell bond between a single cell expressing Ci^{PKA4} and a control neighboring cell. Single cells expressing Ci^{PKA4} were generated by Flp-mediated recombination and are marked by CD8-cherry (red). Laser ablations were performed 5 h after induction of recombination. Adherens junctions are labeled by E-cadherin-GFP (green). Red dots mark ends of ablated cell junctions. (C) Change in distance *d* between the vertices of the indicated cell bonds after ablation as a function of time. Mean and s.e.m. are shown (control bonds, *n*=15 cuts; Ci^{PKA4}, *n*=15 cuts). (D) Initial velocity of vertex displacement after ablation of indicated cell bonds. Mean and s.e.m. are shown (*n* as in C). ***$P<0.001$. (E) Scheme depicting experimental strategy. Two cell bonds along the AP boundary (red line) are ablated subsequently (blue crosses) with a time delay of 20 s. (F-F″) Images from a time-lapse movie (Movie 2) immediately before laser cut and after first and second laser cuts (times in seconds). Adherens junctions are labeled by E-cadherin-GFP and the posterior compartment is identified by expression of GFP-gpi under control of *engrailed* (*en-Gal4*, *UAS-GFP-gpi*). Red dots mark ends of ablated cell junctions. (G) Change in distance *d* between the vertices of cell bonds after first and second cut as a function of time relative to the cut. Mean and s.e.m. are shown (*n*=14 first cuts; *n*=14 second cuts). (H) Initial velocity of vertex displacement after ablation of indicated cell bonds. Mean and s.e.m. are shown. The number of cuts is as in G. n.s., not significant. (I) Scheme detailing the topological changes during a T1 transition. The T1 midline is defined by connecting centroids of a pair of cells that lose contact. The distance *D* between the new junction and the midline is positive when the new junction is located away from the AP boundary and is negative when the new junction is located to the opposite side. The AP boundary is labeled in red. Φ_1 and Φ_2 describe the angles between two junctions right before intercalation. Φ_1 is the angle between two junctions along the AP boundary. Φ_2 is the angle between the two non-AP boundary junctions. (J) Distance *D* of new junctions formed by T1 transitions leading to the intercalation of a cell between two existing cells along the AP boundary for control wing discs and wing discs expressing Ci^{PKA4} in the posterior compartment (*en-Gal4*, *UAS-ci^{PKA}*). Error bars indicate s.e.m. *n*=24 T1 transitions in 5 control wings and *n*=7 T1 transitions in 3 wing discs of the genotype *en-GAL4*, *UAS-ci^{PKA4}*. ***$P<0.001$. (K) Angles Φ_1 and Φ_2 between two cell junctions right before cell intercalation (see I) for the T1 transitions analyzed in J. Error bars indicate s.e.m. ***$P<0.001$; n.s., not significant. The data of control wing discs shown in J and K is based on previously published data (Umetsu et al., 2014).

boundary. We quantified the asymmetry of junctional shrinkage by measuring the position of the new cell junction emerging from the four-way vertex (Fig. 5I). In control wing discs, the new junction was on average positioned closer to the side of the AP boundary (Fig. 5J) (Umetsu et al., 2014), suggesting that the cell junctions shrank predominantly from the vertex located away from the AP boundary. By contrast, in wing discs expressing Ci^{PKA4} in the posterior compartment, the new cell junctions were on average positioned in the center between the pair of cells that lost their junction (Fig. 5J), indicating that the bias in the asymmetry of junctional shrinkage was lost. Comparable observations were made when the angles Φ1 and Φ2 of the cell junctions connected to the four-way vertex were quantified (Fig. 5I,K). Taken together, these data demonstrate that the difference in Hedgehog signal transduction activity between anterior and posterior cells is required to bias the asymmetry of junctional shrinkage during cell intercalations along the AP boundary. Thus, the difference in Hedgehog signal transduction contributes to the characteristic straight shape of the AP boundary by locally increasing cell bond tension, which in turn biases the asymmetry of junctional shrinkage during cell rearrangements.

Differences in Engrailed and Invected expression reduce clonal roughness independently of differences in Hedgehog signal transduction

The maintenance of the straight shape of the AP boundary requires the expression of the homeodomain-containing proteins Engrailed and Invected in posterior cells (Morata and Lawrence, 1975). Engrailed and Invected influence boundary shape by two distinct mechanisms. First, Engrailed and Invected induce expression of Hedgehog in posterior cells and at the same time repress transcription of the transcription factor Ci, which is required for Hedgehog signal transduction, in these cells (Eaton and Kornberg, 1990; Tabata et al., 1992; Zecca et al., 1995). As a consequence,

Development (2015) 142, 3845-3858 doi:10.1242/dev.125542

Hedgehog signal transduction is confined to anterior cells. The experiments described above demonstrate that this difference in Hedgehog signal transduction activity between anterior and posterior cells is necessary to maintain the characteristic straight shape of the AP boundary. Furthermore, previous experiments suggest that Engrailed and Invected maintain the straight shape of the AP boundary by a second mechanism that is independent of Hedgehog signal transduction (Blair and Ralston, 1997; Dahmann and Basler, 2000). This second mechanism has been inferred from experiments, in which mutant clones of cells were generated that differed from their neighboring wild-type cells in the expression of Engrailed and Invected, but not in the activity of Hedgehog signal transduction. Qualitative analyses indicated that such clones display a smooth interface with wild-type cells, indicating that a difference in Engrailed and Invected expression can contribute to the straight shape of the AP boundary independently of differences in Hedgehog signal transduction (Blair and Ralston, 1997; Dahmann and Basler, 2000). To revisit these findings quantitatively, we generated two scenarios in which clones of cells differed in the expression of Engrailed and Invected, but not in Hedgehog signal transduction, from their surrounding wild-type cells and analyzed the clonal roughness of these clones. In scenario I, we sought to eliminate Engrailed and Invected expression in clones of posterior cells that normally express these transcription factors (Fig. 6A). Loss of Engrailed and Invected in posterior cells, however, de-represses Ci and thus activates Hedgehog signal transduction (Eaton and Kornberg, 1990). To prevent the activation of Hedgehog signal transduction, we generated in this scenario I clones of cells triple mutant for *engrailed*, *invected* and *ci* and analyzed such clones located in the posterior compartment. As expected, Engrailed and Ci expression was undetectable in these clones (Fig. S1I,J). The clonal roughness of these clones was intermediate between the clonal roughness of control clones and *engrailed invected* double mutant clones in the posterior compartment (Fig. 6B-E), in which *ci* is de-repressed. These data confirm that differences in the expression of Engrailed and Invected can contribute to smooth clone borders independently of differences in Hedgehog signal transduction. In scenario II, we sought to compare directly the influence of differences in Hedgehog signal transduction and the influence of Hedgehog-independent functions of Engrailed and Invected on clonal shape (Fig. 6F). To this end, we created clones of cells in which the expression of Smoothened (Smo), a protein required to transduce the Hedgehog signal (Alcedo et al., 1996; van den Heuvel and Ingham, 1996), was reduced by RNA interference (RNAi). Similar to mutant smo^{-} clones (Blair and Ralston, 1997; Rodriguez and Basler, 1997), these clones crossed into posterior territory when generated in the anterior compartment close to the AP boundary (Fig. 6H), indicating that Smo function was greatly reduced by RNA interference. The *smo*-RNAi clone border shared with surrounding wild-type anterior cells is a border separating cells with different activities of Hedgehog signal transduction (anterior wild-type cells transduce Hedgehog, whereas clonal cells do not), but not with differences in Engrailed and Invected expression (Engrailed and Invected are not expressed in either cell population). The *smo*-RNAi clone border shared with surrounding wild-type posterior cells, on the contrary, is a border separating cells differing in the expression of Engrailed and Invected (Engrailed and Invected are expressed in posterior cells, but not in clones cells) but not in Hedgehog signal transduction (Hedgehog signal transduction is absent in both cell populations, see Fig. 6F). The clonal roughness of the *smo*-RNAi clone border shared with posterior cells was reduced compared with the clonal roughness of control clones (Fig. 6G,H). Moreover, the clonal roughness of the clone border shared with anterior cells was further reduced compared with the clonal roughness of the clone border shared with posterior cells (Fig. 6G,H). These quantitative analyses confirm that differences in Engrailed and Invected expression between cell populations can lead to smooth boundaries between these cell populations independent of differences in Hedgehog signal transduction. In addition, they suggest that the difference in Hedgehog signal transduction between anterior and posterior cells has a stronger contribution to the straight shape of the AP boundary compared with the difference in Engrailed and Invected expression between anterior and posterior cells.

Differences in Engrailed and Invected expression reduce clonal roughness independently of a local increase in cell bond tension

We next tested whether the difference in Engrailed and Invected expression between anterior and posterior cells locally increases cell bond tension independently of differences in Hedgehog signal transduction. To this end, we ablated cell bonds along borders of *smo*-RNAi clones that were generated in the anterior compartment close to the AP boundary and that had crossed into posterior territory. The vertex distance increase and the initial velocity of displacement upon ablation of clone borders facing wild-type anterior cells were similar to the vertex distance increase and initial velocity of displacement upon ablation of cell bonds along the wild-type AP boundary (Fig. 6I,J; Fig. S3E). Surprisingly, the vertex distance increase and the initial velocity of displacement upon ablation of *smo*-RNAi clone borders facing wild-type posterior cells were similar to the vertex distance increase and the initial velocity of displacement upon ablation of cell bonds between wild-type cells within the compartments (Fig. 6I,J). These results confirm that the difference in Hedgehog signal transduction activity between anterior and posterior cells is sufficient to account for the observed increase in cell bond tension along the AP boundary. More importantly, these data show that the difference of Engrailed and Invected expression between anterior and posterior cells, in the absence of a difference in Hedgehog signal transduction, does not lead to a detectable increase in cell bond tension along the AP boundary. As differences in Engrailed and Invected expression can lead to smooth boundaries in the absence of a local increase in cell bond tension, we conclude that both cell bond tension-dependent and -independent mechanisms contribute to maintenance of the characteristic straight shape of the AP boundary.

DISCUSSION

We have analyzed the links between the determination of cell fate and the physical and mechanical mechanisms shaping the AP boundary of larval *Drosophila* wing discs. Previous work has shown a role for the transcription factors Engrailed and Invected and the Hedgehog signal transduction pathway in organizing the segregation of anterior and posterior cells of the wing disc. We now show that a difference in Hedgehog signal transduction between anterior and posterior cells significantly contributes to the straight shape of the AP boundary by autonomously and locally increasing mechanical cell bond tension that in turn biases the asymmetry of cell rearrangements during cell intercalations. Furthermore, Engrailed and Invected also contribute to maintaining the characteristic straight shape of the AP boundary by mechanisms that are independent of Hedgehog signal transduction and do not appear to modulate cell bond tension.

Development (2015) 142, 3845-3858 doi:10.1242/dev.125542

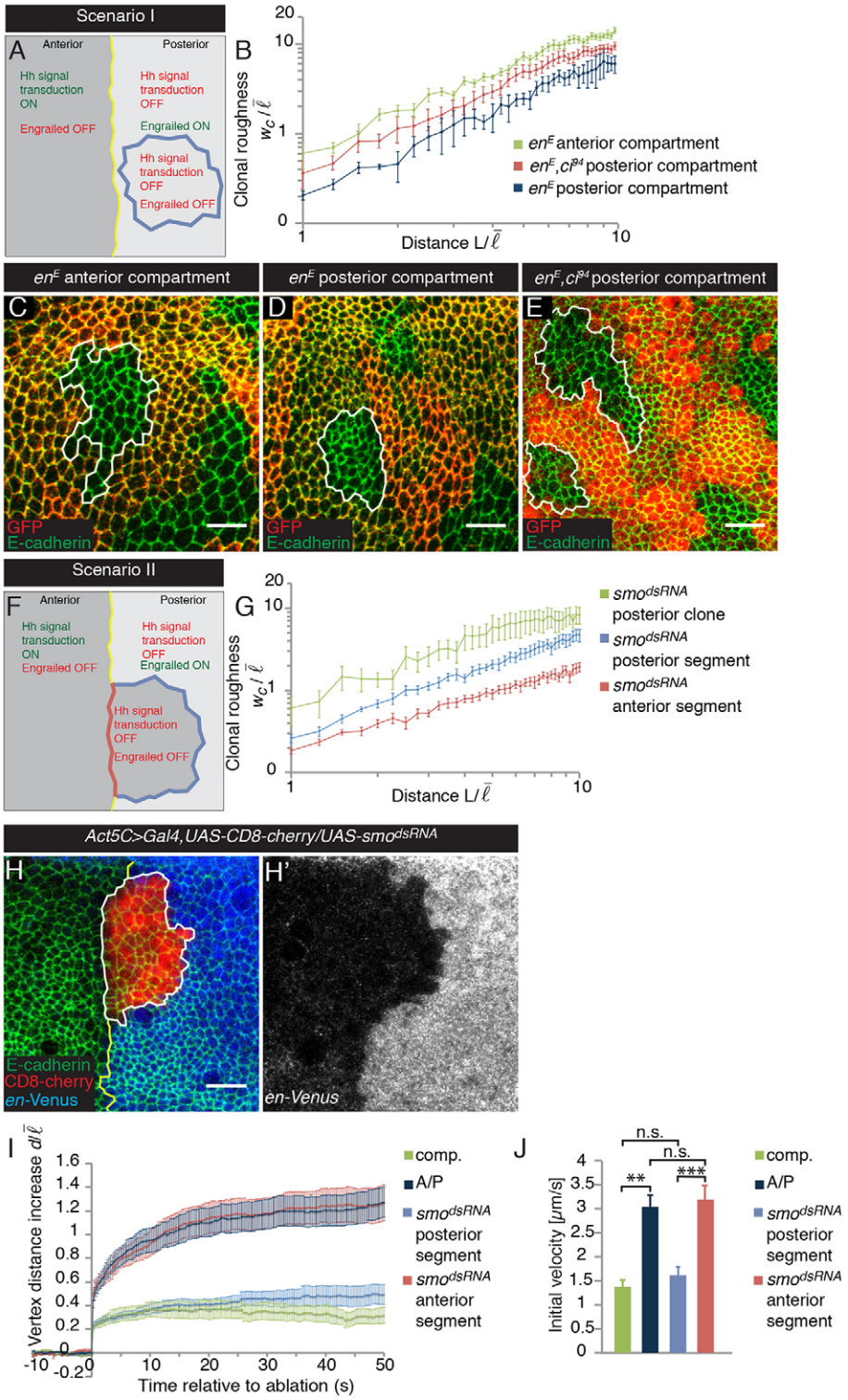

Fig. 6. Engrailed and Invected influence clone shape independently of Hedgehog signal transduction and without modulating cell bond tension. (A) Scheme depicting scenario I (see text for details). The blue line depicts the border of an en^E ci^{94} clone of cells. (B) Clonal roughness w_c as a function of the distance *L* of the borders of en^E mutant clones of cells in the anterior and posterior compartment, and of en^E ci^{94} double mutant clones located in the posterior compartment. en^E mutant clones of cells in the anterior compartment serve as negative control. en^E is a deletion of the *engrailed* and *invected* genes. Mean and s.e.m. are shown (anterior en^E clones, *n*=8; posterior en^E clones, *n*=6; posterior en^E ci^{94} clones, *n*=9). (C-E) Wing discs displaying en^E mutant clones of cells in the anterior (C) and posterior (D) compartment and en^E ci^{94} clones of cells in the posterior compartment (E) marked by the absence of GFP (red). Adherens junctions are labeled by E-cadherin (green). White lines mark the outlines of clones. Scale bars: 10 µm. (F) Scheme depicting scenario II (see text for details). Blue and red lines depict the border of a clone of cells of anterior origin in which the expression of Smo was reduced by RNAi. The blue line indicates the clone border towards posterior cells and the red line the clone border towards anterior cells. (G) Clonal roughness of segments of the borders of clones of cells expressing double-stranded RNA targeting *smo* (smo^{dsRNA}) crossed into the posterior territory facing the anterior (red) or posterior (green) compartments, and of smo^{dsRNA} clones located in the posterior compartment (latter serve as negative control). Mean and s.e.m. are shown (anterior segments of smo^{dsRNA} clones, *n*=6; posterior segments of smo^{dsRNA} clones, *n*=5; posterior smo^{dsRNA} clones, *n*=6). (H,H′) A wing disc displaying a smo^{dsRNA} clone marked by CD8-cherry (red) that crossed from anterior to posterior territory. Adherens junctions are marked by E-cadherin (green) and cells of the posterior compartment are marked by Venus expressed under the *engrailed* enhancer (blue). Scale bar: 10 µm. (I) Change in distance *d* between the vertices of the indicated cell bonds after ablation as a function of time. Mean and s.e.m. are shown (comp., *n*=10; A/P, *n*=12; smo^{dsRNA} posterior segment, *n*=10; smo^{dsRNA} anterior segment, *n*=9 cuts). (J) Initial velocity of vertex displacement after ablation of indicated cell bonds. Mean and s.e.m. are shown. Number of laser cuts as detailed in I. ***P<0.001; **P<0.01; n.s., not significant. The data on cuts within compartments and along the AP boundary shown in I and J are re-plotted from Fig. 4.

A difference in Hedgehog signal transduction results in a cell-autonomous local increase in cell bond tension and a bias in cell rearrangements during cell intercalations

In the wild-type wing disc, anterior cells transducing the Hedgehog signal are juxtaposed to posterior cells that do not transduce the Hedgehog signal. We have generated three cases to test whether this difference in Hedgehog signal transduction is important for the straight shape of the AP boundary, the morphological and molecular signature of cells along the AP boundary, and the local increase in cell bond tension (Fig. 7A-D). In case I, Hedgehog signal transduction was low (or absent) in both A and P cells. In case II, Hedgehog signal transduction was high in both A and P cells. And in case III, Hedgehog signal transduction was high in P cells, but low in A cells, reversing the normal situation. We found that in cases I and II the AP boundary was no longer as straight as in the wild-type situation. Moreover, the increased apical cross-section area of cells along the AP boundary that is characteristic for the wild type was no longer seen. Finally, the levels of F-actin and cell bond

Development (2015) 142, 3845-3858 doi:10.1242/dev.125542

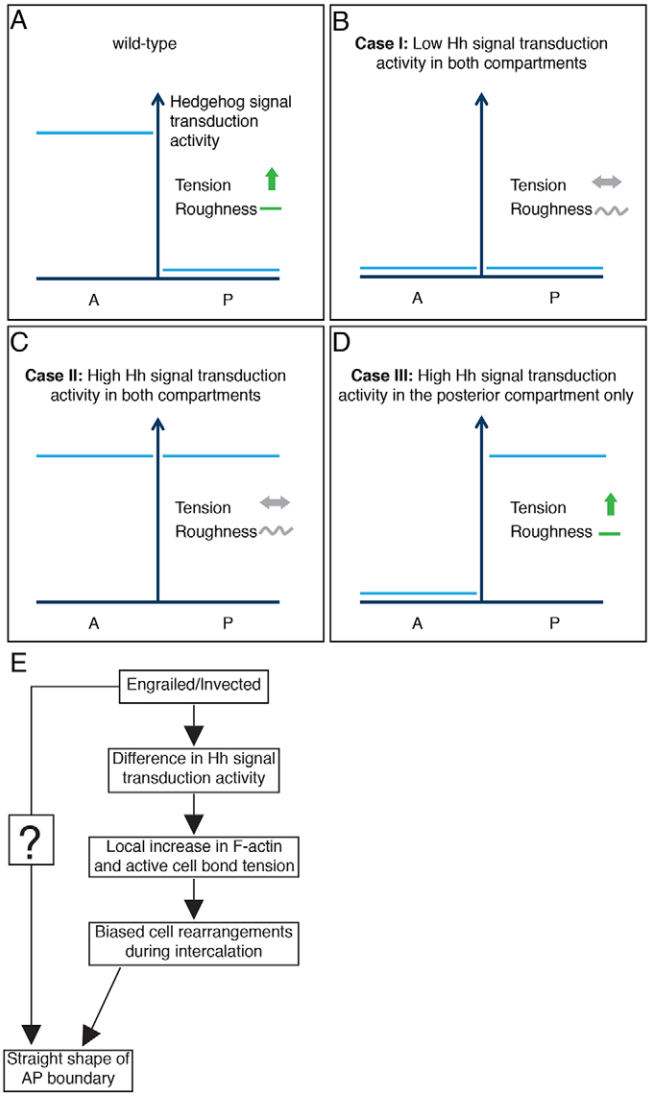

Fig. 7. Summary and model. (A-D) A summary of the results of the different cases to test the role of the difference in Hedgehog signal transduction between anterior and posterior cells for increased cell bond tension along the AP boundary and for the roughness of the AP boundary. (E) Model. The transcription factors Engrailed and Invected promote the straight shape of the AP boundary by two mechanisms. First, they lead to a difference in Hedgehog signal transduction activity between anterior and posterior cells. This difference in Hedgehog signal transduction leads to a local increase of F-actin and active cell bond tension along the AP boundary. The local increase in active cell bond tension biases the asymmetric shrinkage of junctions, resulting in cell rearrangements that keep the straight shape of the AP boundary during cell intercalations. Second, Engrailed and Invected, independently of Hedgehog signal transduction, promote the straight shape of the AP boundary by an unknown mechanism not involving the modulation of cell bond tension.

tension were no longer increased along the AP boundary. In case III, we found that the difference in Hedgehog signal transduction is sufficient to maintain the characteristic straight shape of the AP boundary, to induce the morphological signatures of cells along the AP boundary and to increase F-actin and mechanical tension. Taken together, these experiments establish that the difference in Hedgehog signal transduction between anterior and posterior cells plays a key role in increasing cell bond tension along the AP boundary, in maintaining the characteristic shape of the AP boundary, and in defining the molecular and morphological signatures of cells along the AP boundary. These findings account for the observation that while Hedgehog signal transduction is active within the strip of anterior cells, the increase in mechanical tension is confined to cell bonds along the AP boundary (Landsberg et al., 2009), where cells with highly different Hedgehog signal transduction activities are apposed. The small differences in Hedgehog signal transduction activity that might exist between neighboring rows of anterior cells in the vicinity of the AP boundary appear to be insufficient to increase cell bond tension. Importantly, Hedgehog signal transduction per se does not increase cell bond tension along the AP boundary. The role of Hedgehog signal transduction along the AP boundary thus differs from its roles during other morphogenetic processes in which all cells that transduce the Hedgehog signal, for example, respond by accumulation of F-actin and a change in shape (Corrigall et al., 2007; Escudero et al., 2007). It will be interesting to elucidate the molecular mechanisms by which cells perceive a difference in Hedgehog signal transduction, and how such a difference in Hedgehog signal transduction results in increased cell bond tension.

F-actin and Myosin II are enriched along the AP boundary (Landsberg et al., 2009). Based on similar observations, the existence of actomyosin cables has been proposed for several compartment boundaries, including the AP boundary in the *Drosophila* embryonic epidermis (Monier et al., 2010), the DV boundary of *Drosophila* wing discs (Major and Irvine, 2005, 2006; Monier et al., 2010) and the rhombomeric boundaries in zebrafish embryos (Calzolari et al., 2014). Actomyosin cables have been proposed to maintain the straight shape of compartment boundaries by acting as barriers of cell mixing between cells of the adjacent compartments (Major and Irvine, 2005, 2006; Monier et al., 2010, 2011; Calzolari et al., 2014). Actomyosin cables are also characteristic of additional processes, e.g. dorsal closure and germband extension in the *Drosophila* embryo (Jacinto et al., 2002; Blankenship et al., 2006), tracheal tube invagination and neural plate bending and elongation (Nishimura et al., 2007; Nishimura and Takeichi, 2008), and wound healing (Martin and Lewis, 1992; Wood et al., 2002). During *Drosophila* germ band extension, it has been shown that mechanical tension is higher at cell bonds that are part of an actomyosin cable compared with isolated cell bonds, indicating that cell bond tension is influenced by higher-order cellular organization during this process (Fernandez-Gonzalez et al., 2009). Our results, based on laser ablation experiments, show that the increased cell bond tension along the AP boundary can be induced by single cells and does not depend on the integrity of the actomyosin cable. Thus, our data instead indicate that increased cell bond tension is autonomously generated cell bond by cell bond along the AP boundary. This suggests that differences in Hedgehog signal transduction activity regulate the structure and mechanical properties of cell junctions between adjacent cells and in particular upregulate an active mechanical tension, mediated by actomyosin contractility.

The cell cortex is a thin layer of active material that is under mechanical tension (Prost et al., 2015). In addition to viscous and elastic stresses, active stresses generated by actomyosin contractility are an important contribution. Adherens junctions are adhesive structures that include elements of the cell cortices of the adhering cells (reviewed by Röper, 2015). Locally generated active tension, therefore, can largely determine the cell bond tension as long as cell bonds do not change length or rearrange. As a consequence, locally generated active tension also sets the cell bond tension at the actomyosin cable along the AP boundary. This view is consistent with our experiments in which cell bond tension remains high even

Development (2015) 142, 3845-3858 doi:10.1242/dev.125542

if the integrity of the actomyosin cable is lost. These mechanical properties of cell junctions along the AP boundary are thus different from those of a conventional string or cable in which elastic stresses are associated with stretching deformations. Such elastic stresses relax and largely disappear when the cable is severed. Thus, our work suggests that the mechanical properties of the actomyosin cable along the AP boundary are very different from those of a conventional cable, but fit well in the concepts of active tension studied in the cell cortex, e.g. in *Caenorhabditis elegans* (Mayer et al., 2010). This active tension is a local property that can be set by local signals irrespective of the local force balances. Force balances rather determine movements and rearrangements, e.g. upon laser ablation.

How does a local increase in actively generated cell bond tension contribute to the straight shape of the AP boundary? Our previous work showed that cell intercalations promote irregularities in the shape of compartment boundaries (Umetsu et al., 2014). The local increase in active cell bond tension enters the force balances during cell rearrangements (Umetsu et al., 2014). During cell intercalation, differences in active cell bond tension between junctions along the AP boundary and neighboring junctions are balanced by frictional forces associated with vertex movements. As a result, vertex movements are biased such that the AP boundary remains straight and cell mixing between neighboring compartments is suppressed. The observation that a local difference in Hedgehog signal transduction upregulates active cell bond tension leads to the prediction that cell rearrangements along the AP boundary should not be biased if there is no difference in Hedgehog signal transduction. This is indeed what we found in case II (Fig. 5J,K).

A tension-independent mechanism contributes to the shape of the AP boundary

It has been previously suggested that the *engrailed* and *invected* selector genes play a role in maintaining the separation of anterior and posterior cells that is independent of Hedgehog signal transduction (Blair and Ralston, 1997; Dahmann and Basler, 2000). Our quantitative analysis of clone shapes (Fig. 6) supports this notion. We speculate that this Hedgehog-independent pathway contributes to the remarkably straight shape of the AP boundary in cases I and II, in which Hedgehog signal transduction activities between anterior and posterior cells have been nearly equalized (Figs 1, 2). Two lines of evidence indicate that the Hedgehog-independent pathway shapes the AP boundary without modulating cell bond tension. First, we have generated several cases in which neighboring cell populations differed in the expression of Engrailed and Invected, but not in Hedgehog signal transduction activity (Figs 1, 2; Fig. 6F-J). In none of these cases did we detect an increase in cell bond tension along the interface of these two cell populations. Second, in cases in which we created a difference in Hedgehog signal transduction between two cell populations in the absence of differences in Engrailed and Invected expression (Fig. 6F-J), we detected the same increase in cell bond tension between these cell populations compared with the wild-type compartment boundary.

We have previously described several physical mechanisms that shape the DV boundary of wing discs (Aliee et al., 2012). In addition to a local increase in mechanical tension along the DV boundary, we provided evidence that oriented cell division and cell elongation created by anisotropic stress contribute to the characteristic shape of the DV boundary. It is therefore conceivable that the Hedgehog-independent pathway influences the shape of the AP boundary by one or more of these mechanisms.

A mechano-biochemical process shapes the AP boundary

We propose that the AP boundary is shaped by mechano-biochemical processes that integrate signaling pathways with patterns of cell mechanical properties. In our model, Engrailed and Invected shape the AP boundary with the help of two different mechanisms (Fig. 7E). First, Engrailed and Invected result in a difference in Hedgehog signal transduction between anterior and posterior cells. This difference leads to a cell-autonomous increase in F-actin and active cell bond tension along the AP boundary. The local increase in active cell bond tension then biases the asymmetry of cell rearrangements during cell intercalations and thereby contributes to maintaining the straight shape of the AP boundary. Second, Engrailed and Invected contribute independently of Hedgehog signal transduction to the straight shape of the AP boundary by an as yet unknown mechanism not involving the modulation of cell bond tension. The first mechanism uses biochemical signals to create mechanical patterns that subsequently guide junctional dynamics to organize a straight compartment boundary. We speculate that the second mechanism also involves a mechano-chemical process, even though the nature of this process is currently unknown. Our work suggests that the large-scale shape of the AP boundary thus emerges from the collective behavior of many cells that locally exchange biochemical signals and regulate active mechanical tension.

MATERIALS AND METHODS

Antibody staining

Wing discs were dissected, fixed and stained according to standard protocols (Klein, 2008). Primary antibodies used were mouse anti-β-Galactosidase (Promega Z378A; 1:1000), rat anti-DE-cad [DCAD2, Developmental Studies Hybridoma Bank (DSHB); 1:50], mouse anti-CD2 (AbD, Serotec; 1:1000), rabbit anti-GFP (Santa Cruz Biotechnology sc-8334; 1:2000), mouse anti-Patched, supernatant (Apa1, DSHB; 1:100), mouse anti-Engrailed, supernatant (4D9, DSHB; 1:100) and rat anti-Ci (2A1, DSHB; 1:100). Secondary antibodies were donkey anti-mouse IgG (H+L) Alexa Fluor 555 (Molecular Probes; 1:200), donkey anti-rat Cy5 IgG (H+L) (Jackson ImmunoResearch Laboratories; 1:200) and goat anti-rabbit IgG (H+L) Alexa Fluor 488 (Molecular Probes; 1:200). Alexa Fluor 488 phalloidin (Molecular Probes; 1:200) and rhodamine phalloidin (Molecular Probes; 1:200) were used to detect F-actin.

Image acquisition, processing and analysis

Images of fixed wing discs were acquired on an Olympus FV1000 confocal microscope with a 40×/1.35 NA oil and 60×/1.35 NA oil immersion objective or a Zeiss LSM 780 upright confocal microscope with a 40×/1.4 NA oil immersion objective. *z*-stacks were acquired with a distance of 0.5 µm between images. *z*-stacks were projected by the maximum intensity projection method. Projections were segmented using the custom-made software Packing Analyzer (Aigouy et al., 2010). The region of the AP boundary analyzed corresponds to a range of 42-76 cells for the hh^{ts2}/+ control, 13-49 cells for hh^{ts2}/hh^{ts2}, 37-66 cells for *en-GAL4*, *UAS-*Ci^{PKA4} and 15-26 cells for *en-GAL4*, *UAS-*Ci^{PKA4} hh^{ts2}/hh^{ts2} experiment. The numbers refer to the number of anterior cells along the AP boundary. Angles between neighboring cell bonds, apical cross-section cell area, and F-actin and MRLC-GFP pixel intensities were quantified using Packing Analyzer.

Laser ablation

Laser ablation experiments were performed as described previously (Landsberg et al., 2009). An inverted microscope with a 63×/1.2 NA water immersion objective equipped with a pulsed, third harmonic solid-state UV-laser (355 nm, 400 ps, 20 mJ/pulse) was used.

Culturing of wing discs and analysis of T1 transitions

For the experiments shown in Fig. 5J,K, wing discs of late third instar larvae were cultured as described previously (Zartman et al., 2013). Images were

Development (2015) 142, 3845-3858 doi:10.1242/dev.125542

acquired on a Leica SP5 MP inverse confocal microscope with a 40×/1.25 NA oil immersion objective. T1 transitions were analyzed as described previously (Umetsu et al., 2014).

Statistical analysis

Statistical analysis was performed using a two-sample, unpaired Student's *t*-test.

Acknowledgements

We are grateful to S. Grill for providing us with the laser-ablation system; Benoit Aigouy for implementing the clonal roughness algorithm in Packing Analyzer; and Fabian Hantschke und Felix Philipp Herrmann for help with image segmentation. We thank Marco Milan, Konrad Basler and the Vienna *Drosophila* Resource Center for fly stocks; the Developmental Studies Hybridoma Bank for antibodies; the Light Microscopy Facility at the Center for Regenerative Therapies Dresden (CRTD) for providing imaging equipment; and Christian Bökel and Marcus Michel for critical comments on the manuscript.

Competing interests

The authors declare no competing or financial interests.

Author contributions

K.R., M.A., F.J. and C.D. developed the concepts, K.R. and L.S. performed experiments, K.R., D.U., L.S. and M.A. performed data analysis and C.D. and F.J. prepared the manuscript.

Funding

This work was supported by grants from the Deutsche Forschungsgemeinschaft [DA586/11 and DA586/14 to C.D.].

Supplementary information

Supplementary information available online at
http://dev.biologists.org/lookup/suppl/doi:10.1242/dev.125542/-/DC1

References

Aigouy, B., Farhadifar, R., Staple, D. B., Sagner, A., Röper, J.-C., Jülicher, F. and Eaton, S. (2010). Cell flow reorients the axis of planar polarity in the wing epithelium of Drosophila. *Cell* **142**, 773-786.

Alcedo, J., Ayzenzon, M., Von Ohlen, T., Noll, M. and Hooper, J. E. (1996). The Drosophila *smoothened* gene encodes a seven-pass membrane protein, a putative receptor for the Hedgehog signal. *Cell* **86**, 221-232.

Aliee, M., Röper, J.-C., Landsberg, K. P., Pentzold, C., Widmann, T. J., Jülicher, F. and Dahmann, C. (2012). Physical mechanisms shaping the Drosophila dorsoventral compartment boundary. *Curr. Biol.* **22**, 967-976.

Barabasi, H. L. and Stanley, H. E. (1995). *Fractal Concepts in Surface Growth*. Cambridge: Cambridge University Press.

Basler, K. and Struhl, G. (1994). Compartment boundaries and the control of Drosophila limb pattern by Hedgehog protein. *Nature* **368**, 208-214.

Batlle, E. and Wilkinson, D. G. (2012). Molecular mechanisms of cell segregation and boundary formation in development and tumorigenesis. *Cold Spring Harb. Perspect. Biol.* **4**, a008227.

Blackman, R. K., Sanicola, M., Raftery, L. A., Gillevet, T. and Gelbart, W. M. (1991). An extensive 3′ cis-regulatory region directs the imaginal disk expression of Decapentaplegic, a member of the TGFβ family in Drosophila. *Development* **111**, 657-666.

Blair, S. S. (2003). Developmental biology: boundary lines. *Nature* **424**, 379-381.

Blair, S. S. and Ralston, A. (1997). Smoothened-mediated Hedgehog signalling is required for the maintenance of the anterior-posterior lineage restriction in the developing wing of Drosophila. *Development* **124**, 4053-4063.

Blankenship, J. T., Backovic, S. T., Sanny, J. S. P., Weitz, O. and Zallen, J. A. (2006). Multicellular rosette formation links planar cell polarity to tissue morphogenesis. *Dev. Cell* **11**, 459-470.

Bryant, P. J. (1970). Cell lineage relationships in the imaginal wing disc of Drosophila melanogaster. *Dev. Biol.* **22**, 389-411.

Calzolari, S., Terriente, J. and Pujades, C. (2014). Cell segregation in the vertebrate hindbrain relies on actomyosin cables located at the interhombomeric boundaries. *EMBO J.* **33**, 686-701.

Chen, Y. and Struhl, G. (1996). Dual roles for Patched in sequestering and transducing Hedgehog. *Cell* **87**, 553-563.

Cohen, S. M. (1993). Imaginal disc development. In *The Development of Drosophila melanogaster*, Vol. 2 (ed. M. Bate and A. Martinez Arias) pp. 747-841. New York: Cold Spring Harbor Laboratory Press.

Corrigall, D., Walther, R. F., Rodriguez, L., Fichelson, P. and Pichaud, F. (2007). Hedgehog signaling is a principal inducer of Myosin-II-driven cell ingression in Drosophila epithelia. *Dev. Cell* **13**, 730-742.

Dahmann, C. and Basler, K. (1999). Compartment boundaries: at the edge of development. *Trends Genet.* **15**, 320-326.

Dahmann, C. and Basler, K. (2000). Opposing transcriptional outputs of Hedgehog signaling and Engrailed control compartmental cell sorting at the Drosophila A/P boundary. *Cell* **100**, 411-422.

Dahmann, C., Oates, A. C. and Brand, M. (2011). Boundary formation and maintenance in tissue development. *Nat. Rev. Genet.* **12**, 43-55.

Dominguez, M., Brunner, M., Hafen, E. and Basler, K. (1996). Sending and receiving the Hedgehog signal: control by the Drosophila Gli protein Cubitus interruptus. *Science* **272**, 1621-1625.

Eaton, S. and Kornberg, T. B. (1990). Repression of ci-D in posterior compartments of Drosophila by Engrailed. *Genes Dev.* **4**, 1068-1077.

Escudero, L. M., Bischoff, M. and Freeman, M. (2007). Myosin II regulates complex cellular arrangement and epithelial architecture in Drosophila. *Dev. Cell* **13**, 717-729.

Farhadifar, R., Röper, J.-C., Aigouy, B., Eaton, S. and Jülicher, F. (2007). The influence of cell mechanics, cell-cell interactions, and proliferation on epithelial packing. *Curr. Biol.* **17**, 2095-2104.

Fernandez-Gonzalez, R., Simoes Sde, M., Röper, J.-C., Eaton, S. and Zallen, J. A. (2009). Myosin II dynamics are regulated by tension in intercalating cells. *Dev. Cell* **17**, 736-743.

Forbes, A. J., Nakano, Y., Taylor, A. M. and Ingham, P. W. (1993). Genetic analysis of Hedgehog signalling in the Drosophila embryo. *Dev. Suppl.*, 115-124.

Garcia-Bellido, A., Ripoll, P. and Morata, G. (1973). Developmental compartmentalisation of the wing disk of Drosophila. *Nat. New Biol.* **245**, 251-253.

Garcia-Bellido, A., Ripoll, P. and Morata, G. (1976). Developmental compartmentalization in the dorsal mesothoracic disc of *Drosophila*. *Dev. Biol.* **48**, 132-147.

Hama, C., Ali, Z. and Kornberg, T. B. (1990). Region-specific recombination and expression are directed by portions of the Drosophila *engrailed* promoter. *Genes Dev.* **4**, 1079-1093.

Huang, J., Zhou, W., Dong, W., Watson, A. M. and Hong, Y. (2009). Directed, efficient, and versatile modifications of the Drosophila genome by genomic engineering. *Proc. Natl. Acad. Sci. USA* **106**, 8284-8289.

Irvine, K. D. and Rauskolb, C. (2001). Boundaries in development: formation and function. *Annu. Rev. Cell Dev. Biol.* **17**, 189-214.

Jacinto, A., Wood, W., Woolner, S., Hiley, C., Turner, L., Wilson, C., Martinez-Arias, A. and Martin, P. (2002). Dynamic analysis of actin cable function during Drosophila dorsal closure. *Curr. Biol.* **12**, 1245-1250.

Klein, T. (2008). Immunolabeling of imaginal discs. *Methods Mol. Biol.* **420**, 253-263.

Landsberg, K. P., Farhadifar, R., Ranft, J., Umetsu, D., Widmann, T. J., Bittig, T., Said, A., Jülicher, F. and Dahmann, C. (2009). Increased cell bond tension governs cell sorting at the Drosophila anteroposterior compartment boundary. *Curr. Biol.* **19**, 1950-1955.

Ma, C., Zhou, Y., Beachy, P. A. and Moses, K. (1993). The segment polarity gene *hedgehog* is required for progression of the morphogenetic furrow in the developing Drosophila eye. *Cell* **75**, 927-938.

Major, R. J. and Irvine, K. D. (2005). Influence of Notch on dorsoventral compartmentalization and actin organization in the Drosophila wing. *Development* **132**, 3823-3833.

Major, R. J. and Irvine, K. D. (2006). Localization and requirement for Myosin II at the dorsal-ventral compartment boundary of the Drosophila wing. *Dev. Dyn.* **235**, 3051-3058.

Martin, P. and Lewis, J. (1992). Actin cables and epidermal movement in embryonic wound healing. *Nature* **360**, 179-183.

Martin, A. C. and Wieschaus, E. F. (2010). Tensions divide. *Nat. Cell Biol.* **12**, 5-7.

Mayer, M., Depken, M., Bois, J. S., Jülicher, F. and Grill, S. W. (2010). Anisotropies in cortical tension reveal the physical basis of polarizing cortical flows. *Nature* **467**, 617-621.

McNeill, H. (2000). Sticking together and sorting things out: adhesion as a force in development. *Nat. Rev. Genet.* **1**, 100-108.

Methot, N. and Basler, K. (2000). Suppressor of fused opposes Hedgehog signal transduction by impeding nuclear accumulation of the activator form of Cubitus interruptus. *Development* **127**, 4001-4010.

Monier, B., Pelissier-Monier, A., Brand, A. H. and Sanson, B. (2010). An actomyosin-based barrier inhibits cell mixing at compartmental boundaries in Drosophila embryos. *Nat. Cell Biol.* **12**, 60-65.

Monier, B., Pelissier-Monier, A. and Sanson, B. (2011). Establishment and maintenance of compartmental boundaries: role of contractile actomyosin barriers. *Cell. Mol. Life Sci.* **68**, 1897-1910.

Morata, G. and Lawrence, P. A. (1975). Control of compartment development by the *engrailed* gene in Drosophila. *Nature* **255**, 614-617.

Nishimura, T. and Takeichi, M. (2008). Shroom3-mediated recruitment of Rho kinases to the apical cell junctions regulates epithelial and neuroepithelial planar remodeling. *Development* **135**, 1493-1502.

Nishimura, M., Inoue, Y. and Hayashi, S. (2007). A wave of EGFR signaling determines cell alignment and intercalation in the Drosophila tracheal placode. *Development* **134**, 4273-4282.

Development (2015) 142, 3845-3858 doi:10.1242/dev.125542

Prost, J., Jülicher, F. and Joanny, J.-F. (2015). Active gel physics. *Nat. Phys.* **11**, 111-117.

Rodriguez, I. and Basler, K. (1997). Control of compartmental affinity boundaries by Hedgehog. *Nature* **389**, 614-618.

Röper, K. (2015). Integration of cell-cell adhesion and contractile actomyosin activity during morphogenesis. *Curr. Top. Dev. Biol.* **112**, 103-127.

Schilling, S., Willecke, M., Aegerter-Wilmsen, T., Cirpka, O. A., Basler, K. and von Mering, C. (2011). Cell-sorting at the A/P boundary in the Drosophila wing primordium: a computational model to consolidate observed non-local effects of Hh signaling. *PLoS Comput. Biol.* **7**, e1002025.

Stavans, J. (1993). The evolution of cellular structures. *Rep. Prog. Phys.* **56**, 733-789.

Tabata, T. and Kornberg, T. B. (1994). Hedgehog is a signaling protein with a key role in patterning Drosophila imaginal discs. *Cell* **76**, 89-102.

Tabata, T., Eaton, S. and Kornberg, T. B. (1992). The Drosophila *hedgehog* gene is expressed specifically in posterior compartment cells and is a target of Engrailed regulation. *Genes Dev.* **6**, 2635-2645.

Tepass, U., Godt, D. and Winklbauer, R. (2002). Cell sorting in animal development: signalling and adhesive mechanisms in the formation of tissue boundaries. *Curr. Opin. Genet. Dev.* **12**, 572-582.

Umetsu, D., Aigouy, B., Aliee, M., Sui, L., Eaton, S., Jülicher, F. and Dahmann, C. (2014). Local increases in mechanical tension shape compartment boundaries by biasing cell intercalations. *Curr. Biol.* **24**, 1798-1805.

van den Heuvel, M. and Ingham, P. W. (1996). *smoothened* encodes a receptor-like serpentine protein required for Hedgehog signalling. *Nature* **382**, 547-551.

Vincent, J. P. (1998). Compartment boundaries: where, why and how? *Int. J. Dev. Biol.* **42**, 311-315.

Vincent, J.-P. and Irons, D. (2009). Developmental biology: tension at the border. *Curr. Biol.* **19**, R1028-R1030.

Wood, W., Jacinto, A., Grose, R., Woolner, S., Gale, J., Wilson, C. and Martin, P. (2002). Wound healing recapitulates morphogenesis in Drosophila embryos. *Nat. Cell Biol.* **4**, 907-912.

Zartman, J., Restrepo, S. and Basler, K. (2013). A high-throughput template for optimizing Drosophila organ culture with response-surface methods. *Development* **140**, 667-674.

Zecca, M., Basler, K. and Struhl, G. (1995). Sequential organizing activities of Engrailed, Hedgehog and Decapentaplegic in the Drosophila wing. *Development* **121**, 2265-2278.